Inverse regulation of lipocalin-2/24p3 receptor/Slc22a17 and lipocalin-2 expression by tonicity, Nfat5/TonEBP and arginine vasopressin in mouse cortical collecting duct cells mCCD(cl.1): Implications for osmotolerance

Running title: Osmoregulation of Slc22a17 by Nfat5 & AVP

S. Probst [a*] (Stephanie.Probst@uni-wh.de)

B. Scharner [a*] (Bettina.Scharner@uni-wh.de)

W.-K. Lee [a] (Wing-Kee.Lee@uni-wh.de)

F. Thévenod [a§] (frank.thevenod@uni-wh.de)

Orcid ID Wing-Kee Lee: https://orcid.org/0000-0002-7352-4679

Orcid ID Frank Thévenod: https://orcid.org/0000-0001-8663-3498

Affiliations:

[a] Department of Physiology, Pathophysiology & Toxicology and ZBAF (Centre for Biomedical Education and Research), Faculty of Health, School of Medicine, Witten/Herdecke University, Stockumer Str 12 (Thyssenhaus), D-58453 Witten, Germany

* Authors contributed equally.

§ corresponding author:

- Frank Thévenod, Chair of Physiology, Pathophysiology & Toxicology, Centre for Biomedical Education and Research, Witten/Herdecke University, Germany, frank.thevenod@uni-wh.de

Abstract

The rodent collecting duct (CD) expresses a 24p3/NGAL/lipocalin-2 (Lcn2) receptor (Slc22a17) apically to possibly mediate high-affinity reabsorption of filtered proteins by endocytosis, yet its functions remain uncertain. Recently, we showed that hyperosmolarity/-tonicity upregulates Slc22a17 in cultured mouse inner medullary CD cells, whereas activation of toll-like receptor 4 (TLR4) via bacterial lipopolysaccharides (LPS) downregulates Slc22a17. This is similar to the upregulation of Aqp2 by hyperosmolarity/-tonicity and arginine vasopressin (AVP) and downregulation by TLR4 signaling that occur via the transcription factors Nfat5 (TonEBP or OREBP), cAMP-responsive element binding protein (CREB), and nuclear factor-kappa B, respectively. The aim of the study was to determine the effects of osmolarity/tonicity via Nfat5, AVP via CREB and TLR4 signaling on the expression of Slc22a17 and its ligand Lcn2 in the mouse (m) cortical collecting duct cell line mCCD(cl.1). Normosmolarity/-tonicity was 300 mosmol/l whereas addition of 50-100 mmol/l NaCl for up to 72 h induced hyperosmolarity/-tonicity (400-500 mosmol/l). RT-PCR, qPCR, immunoblotting and immunofluorescence microscopy detected Slc22a17 and Lcn2 expression. RNAi silenced Nfat5, and the pharmacological agent 666-15 blocked CREB. Activation of TLR4 occurred with LPS. Similar to Aqp2, hyperosmotic/-tonic media and AVP upregulated Slc22a17 via activation of Nfat5 and CREB, respectively, and LPS/TLR4 signaling downregulated Slc22a17. Conversely, though Nfat5 mediated hyperosmolarity/-tonicity induced downregulation of Lcn2 expression, AVP reduced Lcn2 expression and predominantly apical Lcn2 secretion evoked by LPS, but through a posttranslational mode of action that was independent of cAMP signaling. In conclusion, the hyperosmotic/-tonic upregulation of Slc22a17 in mCCD(cl.1) cells via Nfat5 and by AVP via CREB suggests a contribution of Slc22a17 to adaptive

osmotolerance, whereas Lcn2 downregulation could counteract increased proliferation and permanent damage of osmotically stressed cells.

Keywords: Kidney; hypertonicity; osmotic stress; lipocalin-2; lipocalin-2 receptor; lipopolysaccharide; TonEBP; CREB.

Introduction

The chief site of urine concentration is in the collecting duct (CD) system [1]. There, the major effector in the regulation of renal water excretion is the antidiuretic hormone arginine vasopressin (AVP) that binds to the AVP type-2 receptor (V2R) and signals through cAMP [2]. In the kidneys, AVP facilitates urinary concentration in the medullary and cortical CD by increasing CD water permeability through enhancement of aquaporin-2 (AQP2) water channel incorporation in the luminal membrane of principal cells, permitting water to flow passively along the osmotic gradient from the tubule lumen to the interstitium [3]. AVP stimulation activates adenylyl cyclase, which results in increased cytosolic cAMP concentration and subsequent protein kinase A (PKA) activation. This, in turn, triggers trafficking of intracellular storage vesicles expressing AQP2 to the luminal plasma membrane within 10-30 minutes (short-term regulation) and also increases AQP2 gene transcription, via increased activity of cAMP-responsive element binding protein (CREB) and AP-1 [4-6], over a time of hours to days (long-term regulation).

For AVP to exert its effects on water transport in the CD, axial cortico-papillary osmotic gradients need to be generated by accumulation of high interstitial concentrations of NaCl (300-400 mmol/l) and urea (> 600 mmol/l) [7, 8]. Na^+ reabsorption in the thick ascending limb results in a renal cortico-papillary osmotic gradient. However, this gradient exposes renal cells to substantial osmotic stress by causing numerous perturbations (reviewed in [9]). Cells can respond to high osmolality stress by activating adaptive mechanisms through various pathways that activate the transcription factor NFAT5 (also known as tonicity-named responsive enhancer binding protein (TonEBP or OREBP)), culminating in accumulation of organic osmolytes and increased expression of heat shock proteins (reviewed in [9]). In addition to AVP, extracellular tonicity is pivotal in determining AQP2 abundance

through activation of NFAT5 that boosts AVP-induced transcriptional activation of AQP2. Conversely, activation of the NF-κB transcriptional factor by pro-inflammatory signals reduces AQP2 gene transcription (reviewed in [3, 10]).

The CD is a site of ascending urinary tract infections (UTI). Lipocalin-2 (Lcn2; also NGAL [human] or siderocalin/24p3 [rodent]) binds Fe^{3+} through association with bacterial siderophores, hence, it plays an important role in antibacterial innate immunity [11]. Activation of the Toll-like receptor 4 (TLR4) on CD cells by the bacterial wall component lipopolysaccharide (LPS) has been shown to induce Lcn2 secretion to combat urinary bacterial infections [12]. A receptor for Lcn2 (Lcn2-R/Slc22a17/24p3-R) has been cloned (MM ~60kDa) [13] and is expressed in the apical membrane of distal convoluted tubules and CD [14]. Experimental evidence in cultured cells and *in vivo* [14, 15] indicates that Slc22a17 is a high-affinity receptor involved in protein endocytosis in the distal nephron [16]. In fact, the affinity of Slc22a17 to proteins, such as Lcn2 or metallothionein, is ~1000x higher than that of megalin [14] (reviewed in [16, 17]), the high-capacity receptor for endocytic reabsorption of filtered proteins in the proximal tubule [18].

Our understanding of the physiological regulation of Slc22a17 and Lcn2 expression *in vivo* is poor. Recent data obtained by deep sequencing in micro-dissected nephrons evidenced the highest Slc22a17 expression levels in the rat inner medullary CD (IMCD) out of all nephron segments whereas Lcn2 levels were negligible [19]. The most abundant localization of Slc22a17 in the CD [14] strongly implies a relationship with the hypertonic environment and possibly regulation by AVP. Our recent data in a mouse IMCD cell line (mIMCD$_3$) cells evidenced Slc22a17upregulation and Lcn2 downregulation induced by hyperosmolarity/-tonicity, suggesting adaptive osmotolerant survival, whereas Lcn2 upregulation and Slc22a17 downregulation via TLR4 indicated protection against bacterial infections [20].

In the present study, the role of increased osmolarity/tonicity on Slc22a17 and Lcn2 expression was investigated in the mouse cortical CD (CCD) cell line mCCD(cl.1). The data indicate that regulation of Slc22a17 expression is analogous to Aqp2, i.e. increased osmolarity/tonicity and AVP induce expression of Slc22a17 via activation of the transcription factors Nfat5 and CREB, respectively, and counteracted by LPS/TLR4 signaling. Whereas Nfat5 mediates Lcn2 downregulation elicited by hyperosmolarity/-tonicity, AVP reduces Lcn2 expression and secretion evoked by LPS through a posttranslational mode of action. The parallel regulation of Aqp2 and Slc22a17 expression in mCCD(cl.1) cells suggests a role of Slc22a17 *in vivo* in urine concentration and/or osmotic stress adaptation.

.

Results

Hyperosmolarity increases the expression of Slc22a17 in mCCD(cl.1) cells

The CD can be separated into the CCD, outer medullary CD (OMCD) and IMCD. Each section of the CD contributes to urine concentration and is also exposed to varying degrees of osmotic stress. As a matter of fact, extracellular osmolarity increases from approximately 300 mosmol/l in the renal cortex to maximally 1200 mosmol/l in the renal medulla. We have previously shown increased extracellular osmolarity augments abundance of the Lcn2 receptor Slc22a17 in a mouse IMCD cell line ($mIMCD_3$) [20]. Slc22a17 is expressed apically along the rodent CD [14] as well as in the mCCD(cl.1) cell line [21]. To assess whether the CCD also harbors a similar positive regulatory relationship between extracellular osmolarity and Slc22a17 expression, mCCD(cl. 1) cells were exposed to hyperosmotic medium and Slc22a17 expression was determined. Indeed, increased osmolarity to 400 mosmol/l for 6 h (*data not shown*) and 12 h induced Slc22a17 mRNA, as demonstrated by RT-PCR (Figure 1A) and qPCR (Figure 1B). Moreover, hyperosmolarity for 48 h increased plasma membrane expression of Slc22a17 protein (Figure 1C). This was associated with increased protein expression of Slc22a17 in microsomes of mCCD(cl.1) cells that are enriched in the plasma membrane-located Na^+/K^+-ATPase (Figure 1D). In addition, Na^+/K^+-ATPase was also upregulated in cells exposed to hyperosmotic media, which indicates an adaptive osmoprotective response to hyperosmolarity has been engaged [9]). In contrast, the ligand of Slc22a17, *Lcn2* was downregulated by hyperosmolarity by RT-PCR (Figure 1E) and qPCR (Figure 1F), which is in line with recent data in $mIMCD_3$ cells [20]. Overall, these data indicate that hyperosmolarity regulates Slc22a17 expression in the CCD cell line mCCD(cl.1) cells whereas the expression of its natural ligand Lcn2 is reduced, recapitulating the same observations made in IMCD cells [20].

Preprints (www.preprints.org) | NOT PEER-REVIEWED | Posted: 4 September 2019 doi:10.20944/preprints201909.0047.v1

Peer-reviewed version available at Int. J. Mol. Sci. 2019, 20, 5398; doi:10.3390/ijms20215398

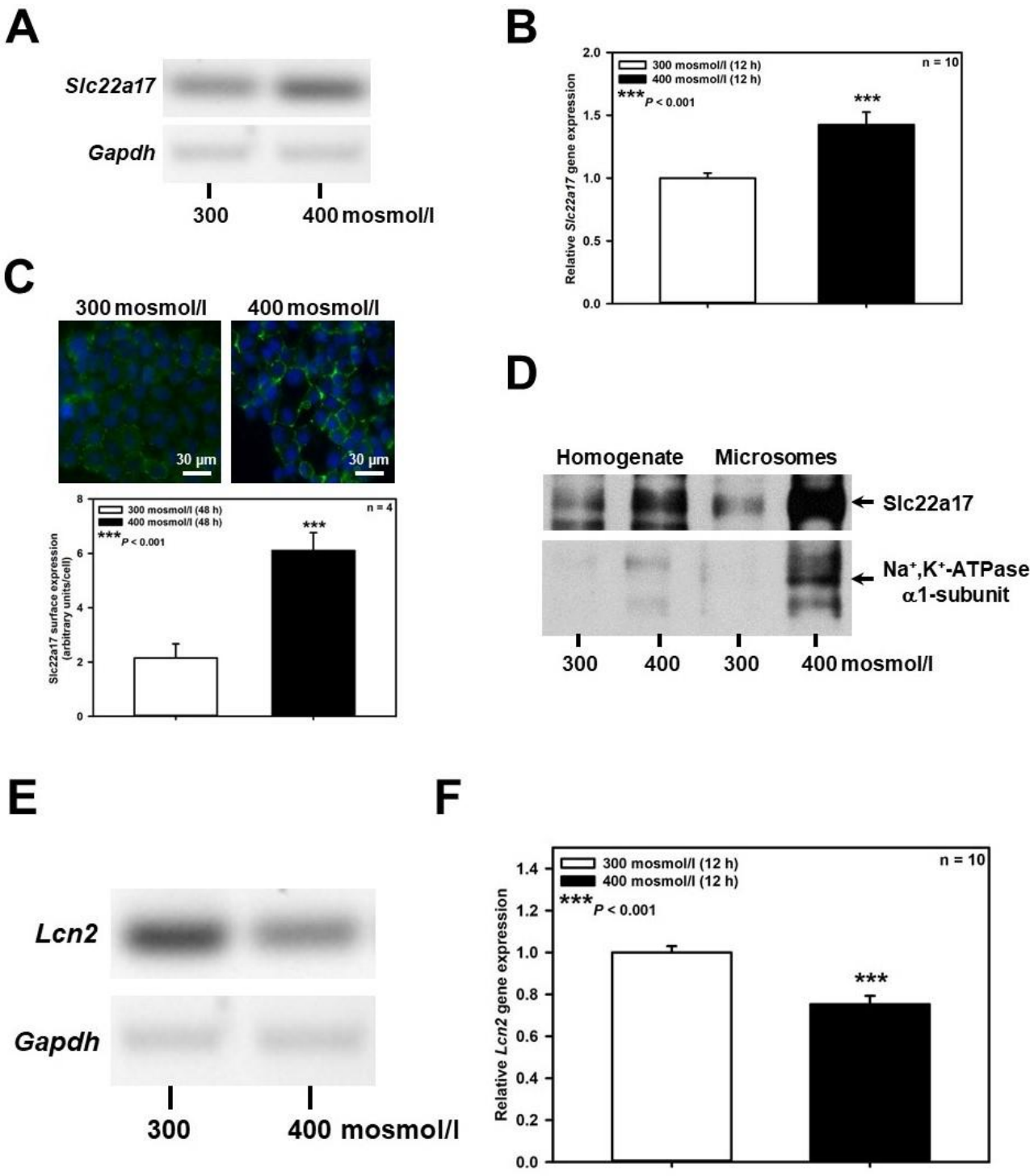

Figure 1. Hyperosmolarity increases Slc22a17 expression and decreases Lcn2 expression in mCCD(cl.1) cells. (**A**) RT-PCR analysis of *Slc22a17* and *Gapdh* mRNA in mCCD(cl.1) cells exposed to 300 mosmol/l (normosmolarity) or 400 mosmol/l (hyperosmolarity) for 12 h. The experiment is typical of three similar ones. (**B**) Expression levels of *Slc22a17* mRNA by qPCR in mCCD(cl.1) cells exposed to norm- or hyperosmotic media for 12 h. Means ± SEM of 10 experiments are shown. Data normalized to the expression of *Gapdh* and *Actb* show relative expression levels of *Slc22a17* under hyperosmotic conditions where expression at 300 mosmol/l is set to 1.0. Statistics compare hyper- to normosmolarity by unpaired *t*-test. (**C**) Surface expression of Slc22a17 in mCCD(cl.1) cells exposed to norm- or hyperosmotic media for 48 h. Slc22a17 is detected by live immunofluorescence microscopy of non-fixed and non-permeabilized cells with a Slc22a17 antibody directed against the extracellular N-terminus. Hoechst 33342 counterstains nuclei. Means ± SEM of 4 experiments are shown and comparison of the

two osmotic conditions by unpaired *t*-test. a.u. = arbitrary units. (**D**) Immunoblotting of homogenate and microsomes enriched in plasma membranes from mCCD(cl.1) cells grown for 72 h in norm- or hyperosmotic media. Slc22a17 is at the expected molecular mass of ~62 kDa. The α1-subunit of Na^+,K^+-ATPase, a plasma membrane marker, is enriched in microsomes and upregulated in cells exposed to hyperosmolarity. The experiment is representative of three similar ones. (**E**) RT-PCR analysis of *Lcn2* and *Gapdh* mRNA in mCCD(cl.1) cells exposed to 300-400 mosmol/l media for 12 h. The experiment is typical of three similar ones. (**F**) Expression levels of *Lcn2* mRNA by qPCR in mCCD(cl.1) cells exposed to 300-400 mosmol/l media for 12 h. Means ± SEM of 10 experiments are shown. Data normalized to the expression of *Gapdh* and *Actb* show relative expression levels of *Slc22a17* under hyperosmotic conditions where expression at 300 mosmol/l is set to 1.0. Statistics compare the two osmotic conditions by unpaired *t*-test.

Hypertonicity dependent upregulation of Slc22a17 and downregulation of Lcn2 are mediated by Nfat5 in mCCD(cl.1) cells

Increased extracellular osmolarity has previously been shown to increase abundance of the water channel Aqp2 *in vivo* [22, 23] and in the mouse renal CD principal cell line mpkCCDcl4 (reviewed in [3, 10]), and depends on increased nuclear activity of the transcription factor Nfat5 (TonEBP/OREBP) [24], which is also affected by osmolarity *in vivo* [25]. These findings were confirmed in the mCCD(cl.1) cell line: hyperosmolarity up to 500 mosmol/l for 24 h upregulated *Aqp2* mRNA by RT-PCR (Figure 2A) and qPCR (Figure 2B), slightly increased Nfat5 (Figure 2C), suggesting slow induction of Nfat5 protein [26, 27], and induced translocation of cytosolic Nfat5 to nuclei (Figure 2D). To investigate whether the upregulation of Aqp2 by hyperosmolarity is also mediated by Nfat5 in mCCD(cl.1) cells, RNAi was performed using siRNAs against *Nfat5*, which efficiently abolished hyperosmolarity-induced increase in *Nfat5* at both the mRNA (Figure 2E) and protein (Figure 2C) levels. Accordingly, as expected *Nfat5* silencing almost abolished induction of *Aqp2* mRNA elicited by hyperosmolarity (Figure 2F).

Preprints (www.preprints.org) | NOT PEER-REVIEWED | Posted: 4 September 2019 doi:10.20944/preprints201909.0047.v1

Peer-reviewed version available at Int. J. Mol. Sci. 2019, 20, 5398; doi:10.3390/ijms20215398

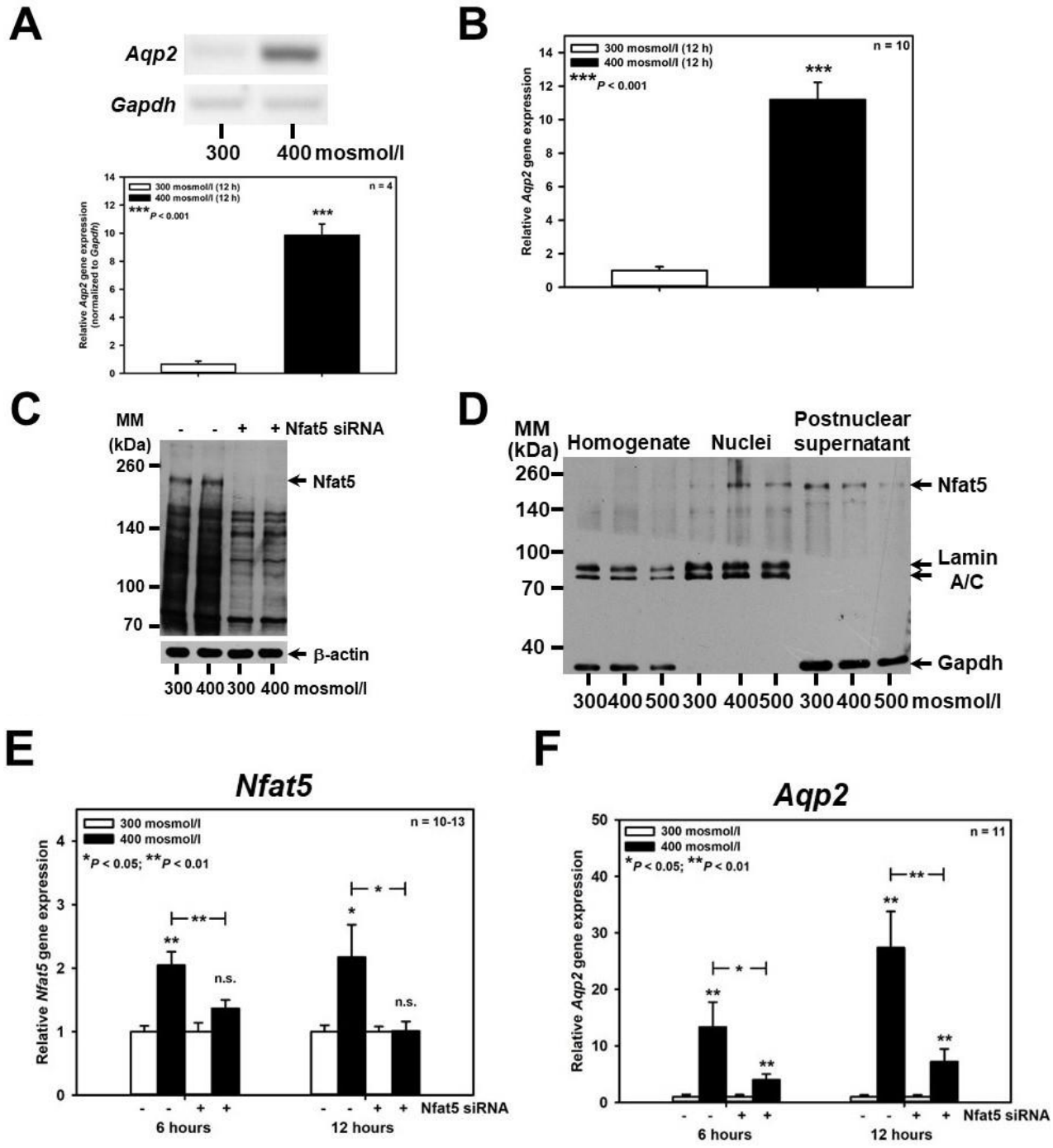

Figure 2. Aqp2 upregulation induced by hyperosmolarity is mediated by Nfat5 in mCCD(cl.1) cells. (**A**) Expression levels of *Aqp2* mRNA by RT-PCR in mCCD(cl.1) cells exposed to 300-400 mosmol/l for 12 h. *Aqp2* mRNA expression was normalized to *Gapdh*, and expression levels at 300 mosmol/l are set to 1.0. Data show means ± SEM of 4 experiments. Statistical analysis compares hyper- to normosmolarity by unpaired *t*-test. (**B**) Expression levels of *Aqp2* mRNA by qPCR in mCCD(cl.1) cells exposed to 300-400 mosmol/l. Means ± SEM of 10 experiments are shown. Data normalized to the expression of *Gapdh* and *Actb* show relative expression levels of *Slc22a17* under hyperosmotic conditions where expression at 300 mosmol/l is set to 1.0. Statistics compare hyper- to normosmolarity by unpaired *t*-test. (**C**, **F**) mCCD(cl.1) cells are transfected with siRNA against *Nfat5* or control siRNA by electroporation. Then cells are seeded in 25 cm^2 flasks and grown for 24 h prior to medium change to 300 and 400 mosmol/l and incubation for additional 6-12 h. Expression levels of *Nfat5* (**C**) and *Aqp2* mRNA (**F**) are determined by qPCR, as described above. Statistical analysis shows means ± SEM of 10-13 experiments and compares the experimental conditions by one-way ANOVA. n.s. = not significant. (**D**) Distribution of

Nfat5 in homogenate, nuclei and postnuclear supernatant of mCCD(cl.1) cells exposed to 300-500 mosmol/l for 24 h prior to homogenization, subcellular fractionation and immunoblotting of Nfat5. Lamin A/C and Gapdh are markers of nuclei and cytosol, respectively. The immunoblot is typical for three different blots. MM = molecular mass. (**E**) mCCD(cl.1) cells were transfected with control or *Nfat5* siRNA by electroporation and cultured, as described above prior to medium change to 300 and 400 mosmol/l for additional 24 h and immunoblotting. β-actin serves as a loading control. The blot is typical for three similar ones. MM = molecular mass.

As the central response pathway to changes in tonicity, we hypothesized that Slc22a17 and its ligand Lcn2 could be regulated by Nfat5 when extracellular osmolarity rises. Strikingly, induction of Slc22a17 mRNA by hyperosmolarity was significantly reduced by Nfat5 silencing after 6-12 h (Figure 3A), and expression of Slc22a17 protein at the surface of mCCD(cl.1) cells was significantly decreased after 24 h hyperosmolarity (Figure 3B). In contrast, Nfat5 silencing reversed downregulation of Lcn2 mRNA expression induced by hyperosmolarity. Figure 3C shows that hyperosmolarity induced an early decrease of Lcn2 mRNA at 6 and 12 h, which was significantly reversed by Nfat5 silencing at 6 h, and confirmed at the protein level by immunoblotting of Lcn2 (Figure 3D). Hence, the transcription factor Nfat5, which regulates the expression of genes involved in the osmotic stress, is largely responsible for up- and downregulation of Slc22a17 and Lcn2, respectively.

Preprints (www.preprints.org) | NOT PEER-REVIEWED | Posted: 4 September 2019 doi:10.20944/preprints201909.0047.v1

Peer-reviewed version available at Int. J. Mol. Sci. 2019, 20, 5398; doi:10.3390/ijms20215398

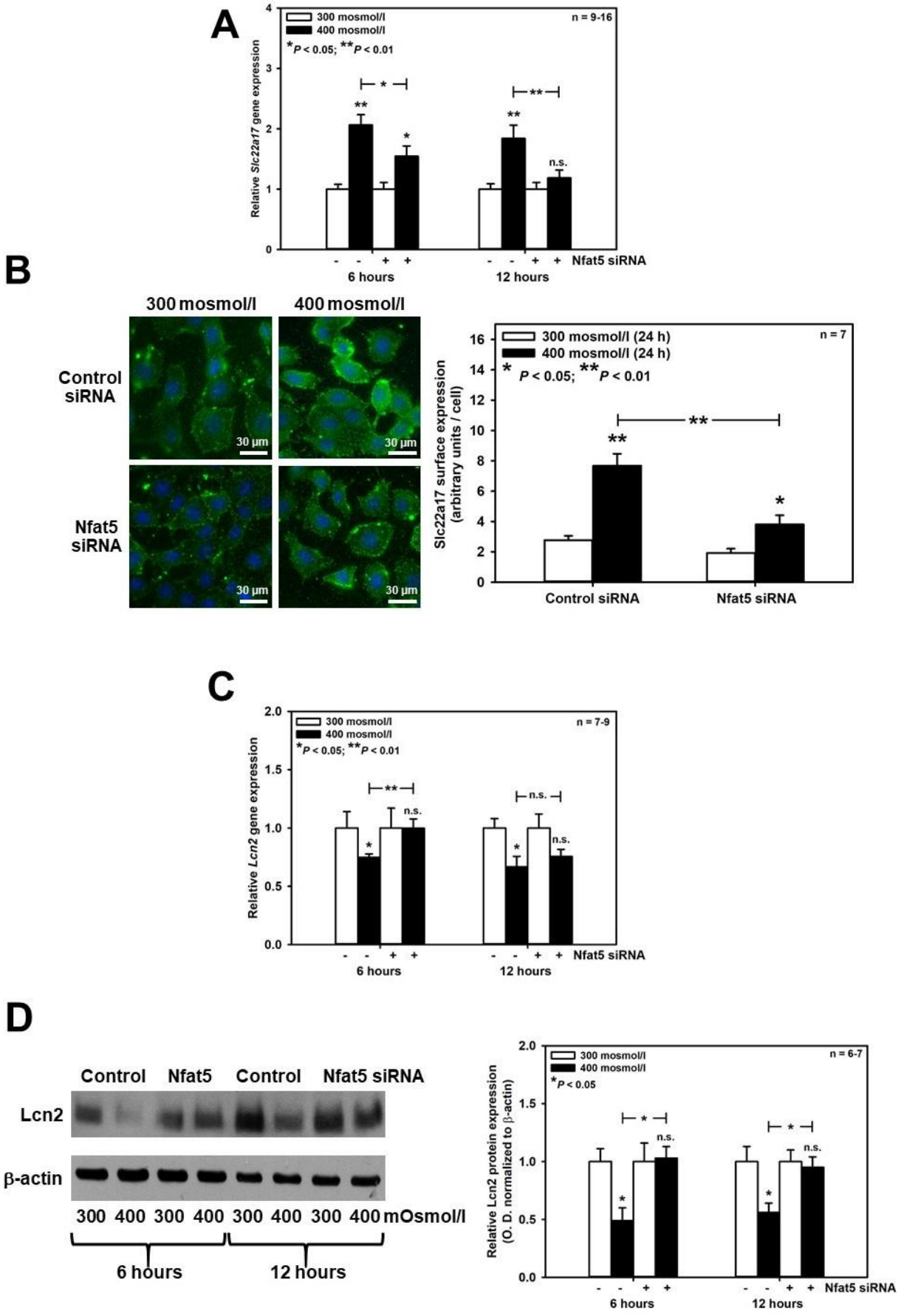

Figure 3. Nfat5 mediates the effects of hyperosmolarity on Slc22a17 and Lcn2 expression in mCCD(cl.1) cells. (**A**, **C**) mCCD(cl.1) cells were transfected with control or *Nfat5* siRNA by

electroporation and cultured as described in the *Methods*, prior to medium change to 300 and 400 mosmol/l and incubation for additional 6-12 h. Expression levels of *Slc22a17* (**A**) and *Lcn2* (**C**) mRNA were detected by qPCR, as described in Figure 1. Statistical analysis shows means ± SEM of 7-16 experiments and compares the experimental conditions by one-way ANOVA. n.s. = not significant. (**B**) Surface expression of Slc22a17 was determined in mCCD(cl.1) cells transfected with siRNA against *Nfat5* or control siRNA by electroporation. Cells are exposed to 300 and 400 mosmol/l for additional 24 h. Plasma membrane Slc22a17 is detected as described in Figure 1. Hoechst 33342 counterstains nuclei. Statistical analysis shows means ± SEM of 7 experiments and compares the experimental conditions by one-way ANOVA. n.s. = not significant. (**D**) Immunoblotting of cellular Lcn2 protein in mCCD(cl.1) cells transfected with siRNA against *Nfat5* or control siRNA by electroporation. Incubation of cells occurs in 300 and 400 mosmol/l media for additional 6-12 h prior to immunoblotting. Data show cellular Lcn2 protein expression normalized to β-actin as means ± SEM of 6-7 experiments, where expression at 300 mosmol/l is set to 1.0. Statistical analysis compares the experimental conditions by one-way ANOVA. n.s. = not significant.

ddAVP upregulates Slc22a17 via cAMP/CREB signaling in mCCD(cl.1) cells

In addition to hyperosmolarity, the V2R also increases AQP2 protein abundance to facilitate urinary concentration in the CCD and MCD [28, 29] through an cAMP-responsive element (CRE) located in the AQP2 promoter, leading to AVP-induced AQP2 transcription [4-6]. This mechanism has been reported in mpkCCDcl4 cells [30, 31]. Analogously, when mCCD(cl.1) cells were exposed to the specific V2R agonist ddAVP (10 nM) for 24 h in isotonic medium, *Aqp2* mRNA was increased 5.85 ± 0.71-fold, and this effect was significantly reduced to 2.60 ± 0.29 (means ± SEM of 7-11 experiments) by the potent inhibitor of CREB-mediated gene transcription, 666-15 (100-250 nM) [32] (Figure 4A). Noticeably, ddAVP slightly, but significantly upregulated *Slc22a17* mRNA (1.38 ± 0.06-fold; n = 7-11) in a 666-15 sensitive-manner (Figure 4A). The latter results were further confirmed at the protein level by quantifying surface expression of Slc22a17 protein in mCCD(cl.1) cells treated exactly as described for the qPCR data shown in Figure 4A. Figure 4B shows that ddAVP increased Slc22a17 surface expression about 2-fold, and a role for CREB activation was demonstrated by a significant reduction in Slc22a17 surface expression by preincubation with 666-15 (Figure 4B). Consequently, gene regulatory mechanisms for Slc22a17 via the

transcription factors Nfat5 and CREB in response to osmotic stress parallels that of Aqp2.

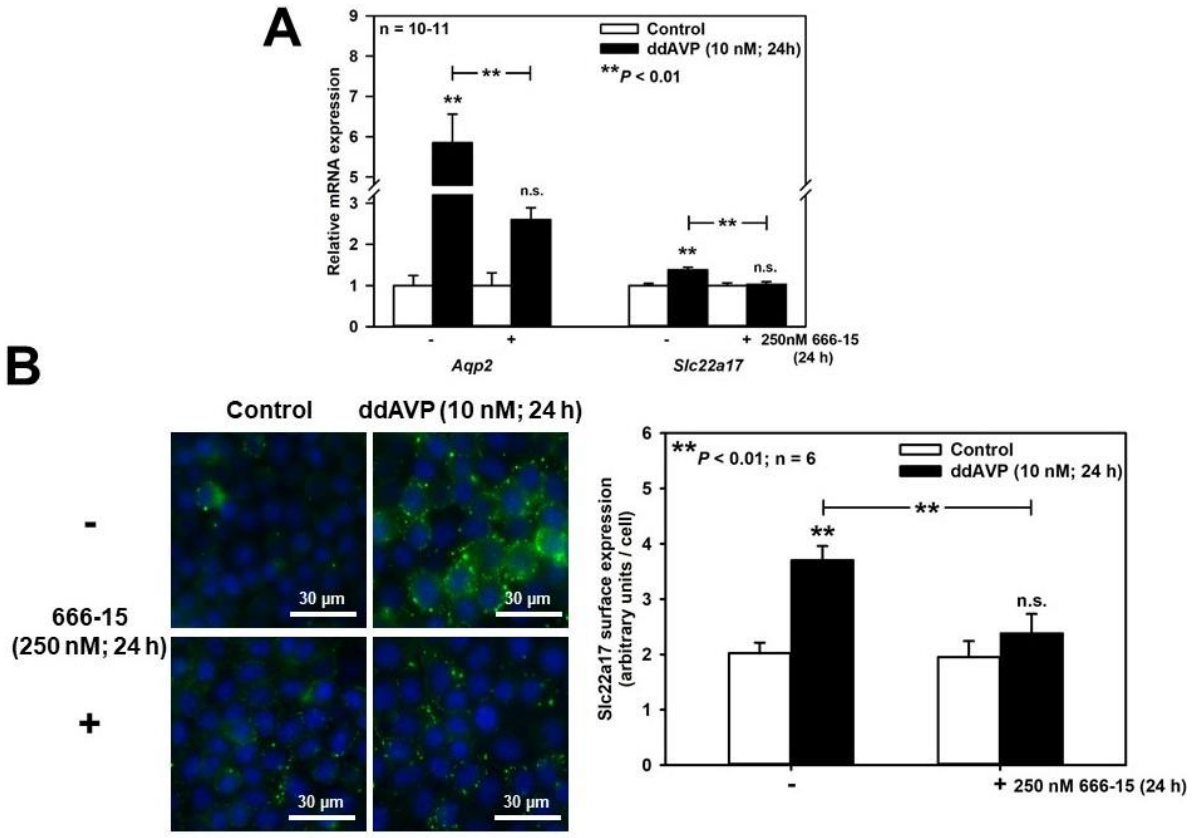

Figure 4. ddAVP increases Slc22a17 expression through CREB activation in mCCD(cl.1) cells. (**A**) Expression levels of *Aqp2* and *Slc22a17* mRNA by qPCR in cells treated with ddAVP ± the CREB inhibitor 666-15 and analyzed and calculated, as described in Figure 1. Data are means ± SEM of 10-11 experiments. Statistical analysis compares relative expression levels of *Aqp2* or *Slc22a17* in controls and ddAVP-treated cells ± 666-15 by one-way ANOVA. n.s. = not significant. (**B**) Surface expression of Slc22a17 in cells treated with ddAVP ± 666-15. Staining of non-fixed and non-permeabilized cells grown on glass coverslips was performed using a Slc22a17 antibody directed against the extracellular N-terminus. Hoechst 33342 counterstains nuclei. Statistical analysis shows means ± SEM of 6 experiments and compares the four experimental conditions by one-way ANOVA. n.s. = not significant.

LPS downregulates Slc22a17 and upregulates Lcn2 in mCCD(cl.1) cells

The renal CD is susceptible to bacterial infections that can ascend from the lower urinary tract during UTIs. Activation of TLR4 [33] in collecting ducts [34] mediated by NF-κB-mediated signaling [35, 36] via bacterial LPS has been previously shown in our earlier work to induce Lcn2 upregulation and Slc22a17 downregulation in mIMCD3 cells and suggested to protect IMCD cells against bacterial infections and prevent autocrine death induction by Lcn2 [20]. Here we investigated whether LPS also inhibits

Slc22a17 expression in the CCD. When mCCD(cl.1) cells incubated in isotonic medium were exposed to LPS (5 µg/ml) for 12 h, *Slc22a17* mRNA was significantly reduced (Figure 5A), as measured by RT-PCR. Similarly, LPS reduced cellular and surface expression of Slc22a17 as well (Figure 5B). LPS at 100 ng/ml for 12 h yielded similar results.

Further corroborating our previous findings in IMCD, LPS (5 µg/ml for 12 h) significantly stimulated Lcn2 mRNA expression in mCCD(cl.1) cells (Figure 5C) and increased Lcn2 protein expression when cells were exposed for 18 h to 5 µg/ml LPS (Figure 5D and 5E). Interestingly, LPS exposure time ≤ 12 h marginally increased Lcn2 secretion. Secretion of Lcn2 occurred predominantly apically, when LPS was applied to both, the apical and basolateral compartments of confluent monolayers of mCCD(cl.1) cells grown on transwell filters (Figure 5E). Yet, unstimulated secretion was also predominantly apical (Figure 5E), confirming that constitutive as well as regulated Lcn2 secretion is largely targeted to the apical plasma membrane, as previously suggested [12].

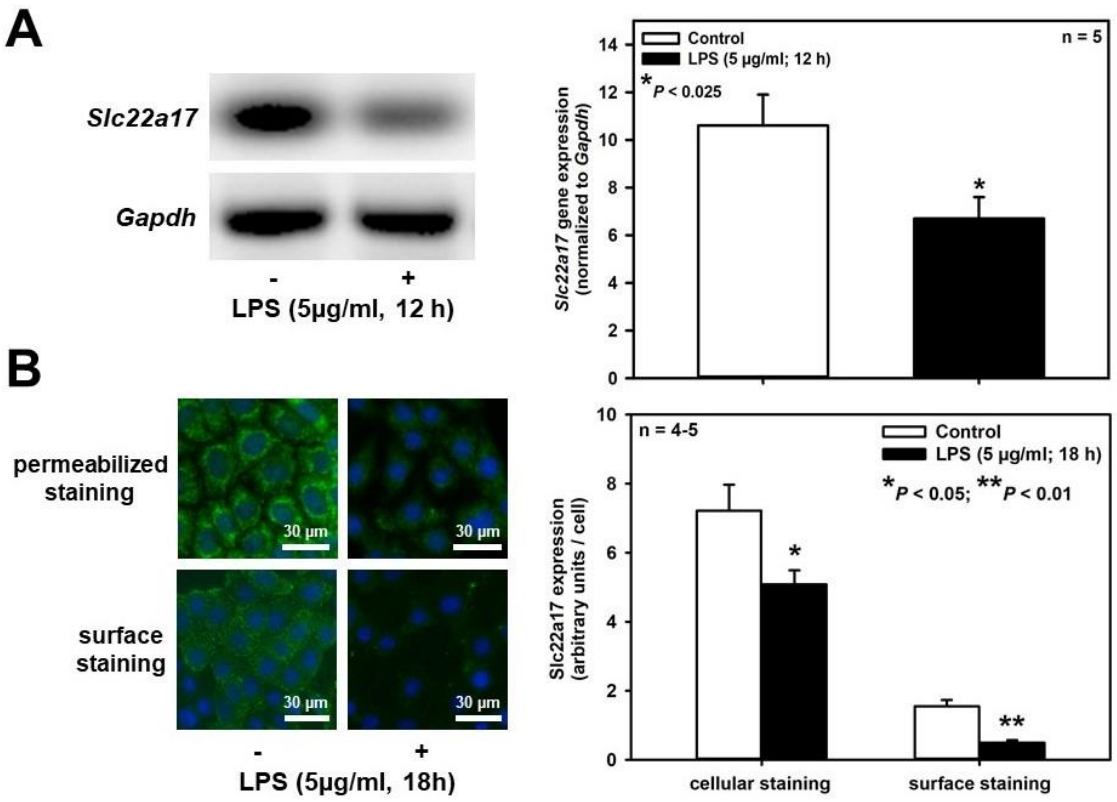

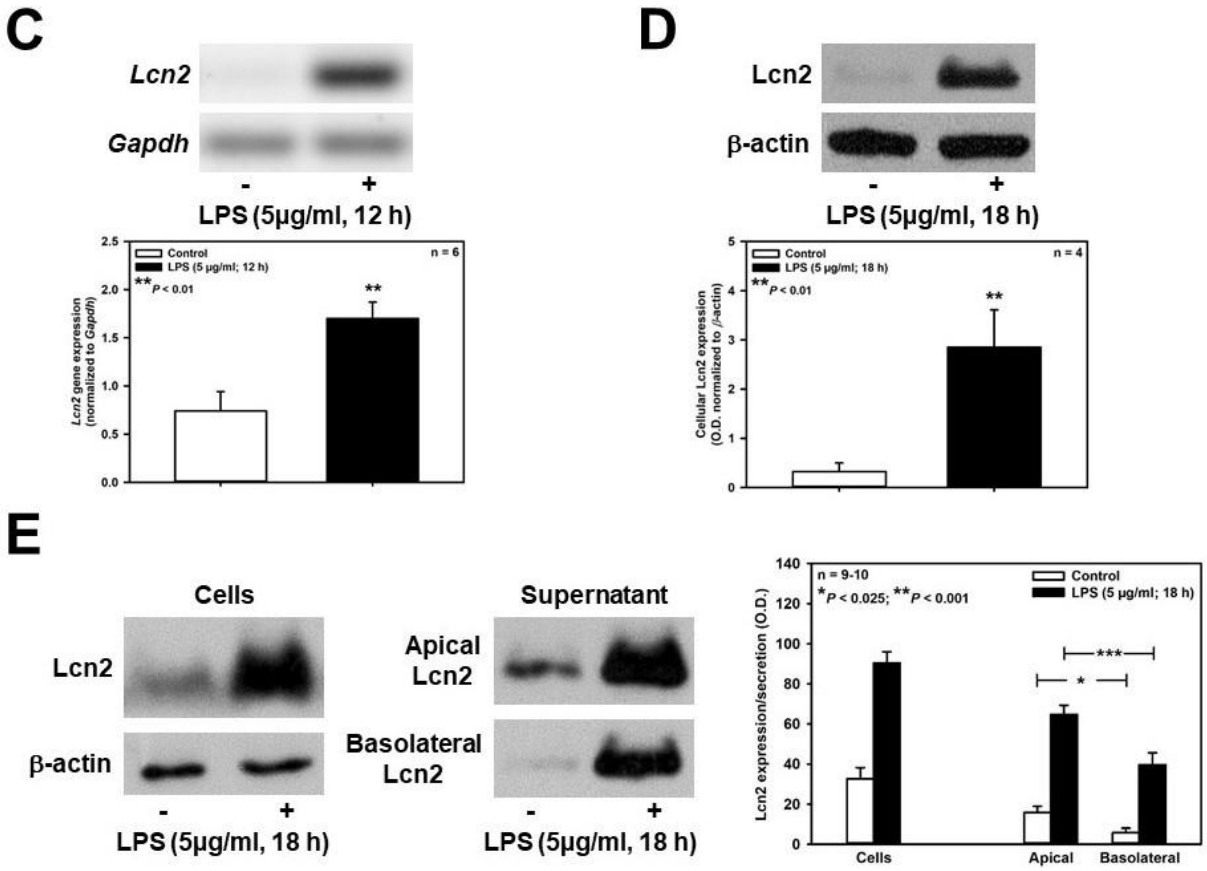

Figure 5. LPS decreases Slc22a17 expression and increases Lcn2 expression in mCCD(cl.1) cells. (**A**) Expression levels of *Slc22a17* mRNA by RT-PCR in mCCD(cl.1) cells treated with 5 µg/ml lipopolysaccharides (LPS) for 12 h. *Slc22a17* mRNA expression was normalized to *Gapdh*. Data show means ± SEM of 5 experiments. Statistical analysis compares the effects of control versus LPS by unpaired *t*-test. (**B**) Expression of Slc22a17 in mCCD(cl.1) cells treated with 5 µg/ml LPS for 18 h was detected by immunofluorescence microscopy of permeabilized and non-permeabilized (cell surface expression) cells using a Slc22a17 antibody directed against the extracellular N-terminus. Hoechst 33342 counterstains nuclei. Statistical analysis shows means ± SEM of 4-5 experiments and comparison of the two conditions by unpaired *t*-test. (**C**) Expression levels of *Lcn2* mRNA by RT-PCR in mCCD(cl.1) cells treated with LPS. *Lcn2* mRNA expression was normalized to *Gapdh*. Data show means ± SEM of 6 experiments. Statistical analysis compares the effects of control versus LPS by unpaired *t*-test. (**D**) Effect of LPS on expression of Lcn2 protein in mCCD(cl.1) cells. Cellular Lcn2 protein expression was normalized to β-actin. Data show means ± SEM of 4 experiments. Statistical analysis determines the effect of LPS on cellular Lcn2 protein using unpaired *t*-test. (**E**) Effect of LPS on cellular expression and secretion of Lcn2 protein in mCCD(cl.1) cell monolayers grown to confluence on transwell filters. LPS or solvent were applied to both apical and basolateral chambers for 18 h. Cells were lysed, whereas apical and basolateral media were collected and concentrated to the same volume, as described in the "methods". Corresponding corrected volumes of concentrated media were loaded for immunoblotting. Data show cellular Lcn2 protein expression normalized to β-actin as means ± SEM of 9-10 experiments. Statistical analysis determines the effect of LPS on cellular and apically or basolaterally secreted Lcn2 protein using by one-way ANOVA.

ddAVP posttranslationally downregulates unstimulated and LPS-stimulated Lcn2 in mCCD(cl.1) cells

As shown in Figure 6A, LPS (5 µg/ml for 18 hours) significantly reduces unstimulated and ddAVP-induced *Aqp2* mRNA expression in mCCD(cl.1) cells, thus confirming previous studies in mpkCCDcl4 cells [35]. Despite LPS stimulation of *Lcn2* mRNA levels (Figure 6B), ddAVP (10 nM) had no effect on Lcn2 mRNA, which was confirmed by qPCR (Figure 6C). In addition, the CREB inhibitor 666-15 was ineffective (Figure 6C). Quite surprisingly, and in contrast to the mRNA data, both unstimulated and LPS-stimulated Lcn2 protein expression and secretion were reduced by ddAVP (Figure 6D), suggesting a posttranslational effect of ddAVP on Lcn2 expression and secretion. Indeed, co-application of cycloheximide (0.01 µg/ml for 3-6 h), a blocker of translational elongation [37], prevented downregulation of Lcn2 protein expression induced by ddAVP (Figure 6E), which indicates that ddAVP promotes Lcn2 degradation following protein translation.

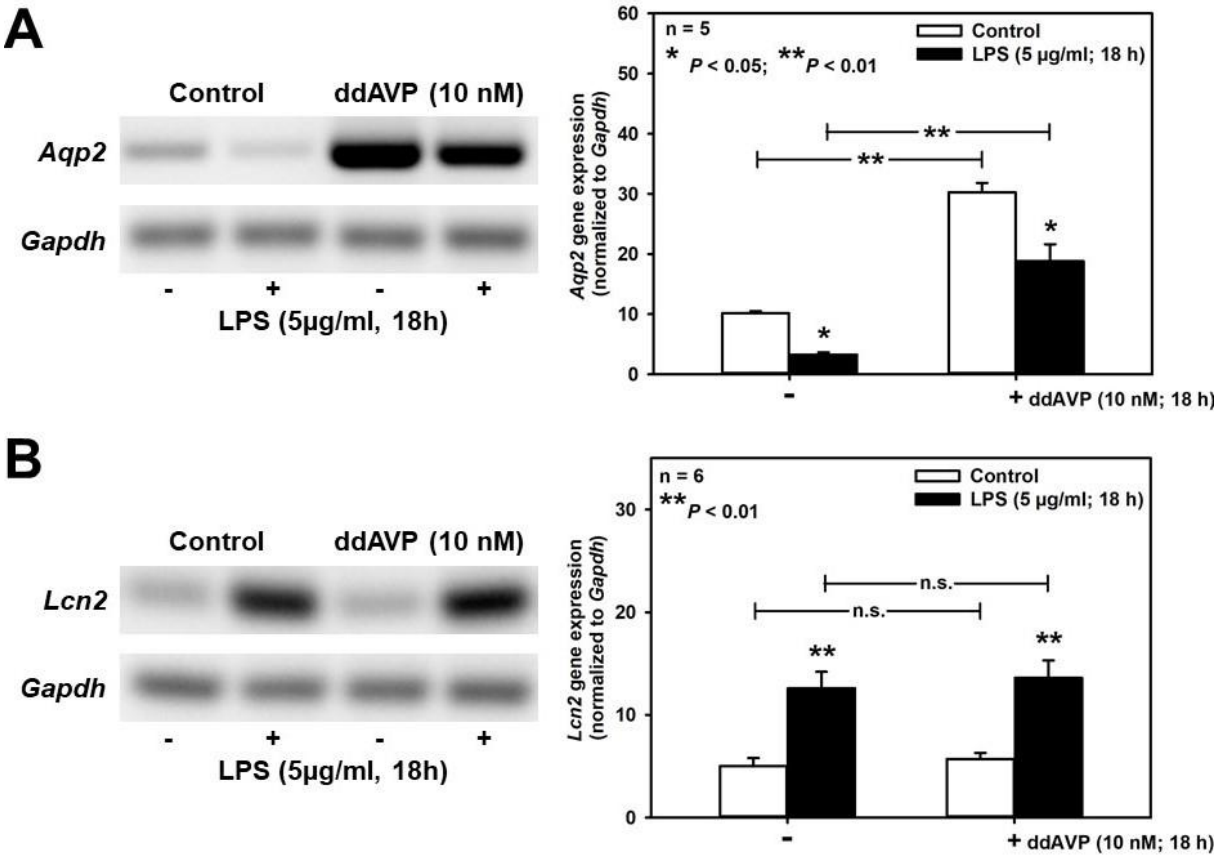

Preprints (www.preprints.org) | NOT PEER-REVIEWED | Posted: 4 September 2019 doi:10.20944/preprints201909.0047.v1

Peer-reviewed version available at Int. J. Mol. Sci. 2019, 20, 5398; doi:10.3390/ijms20215398

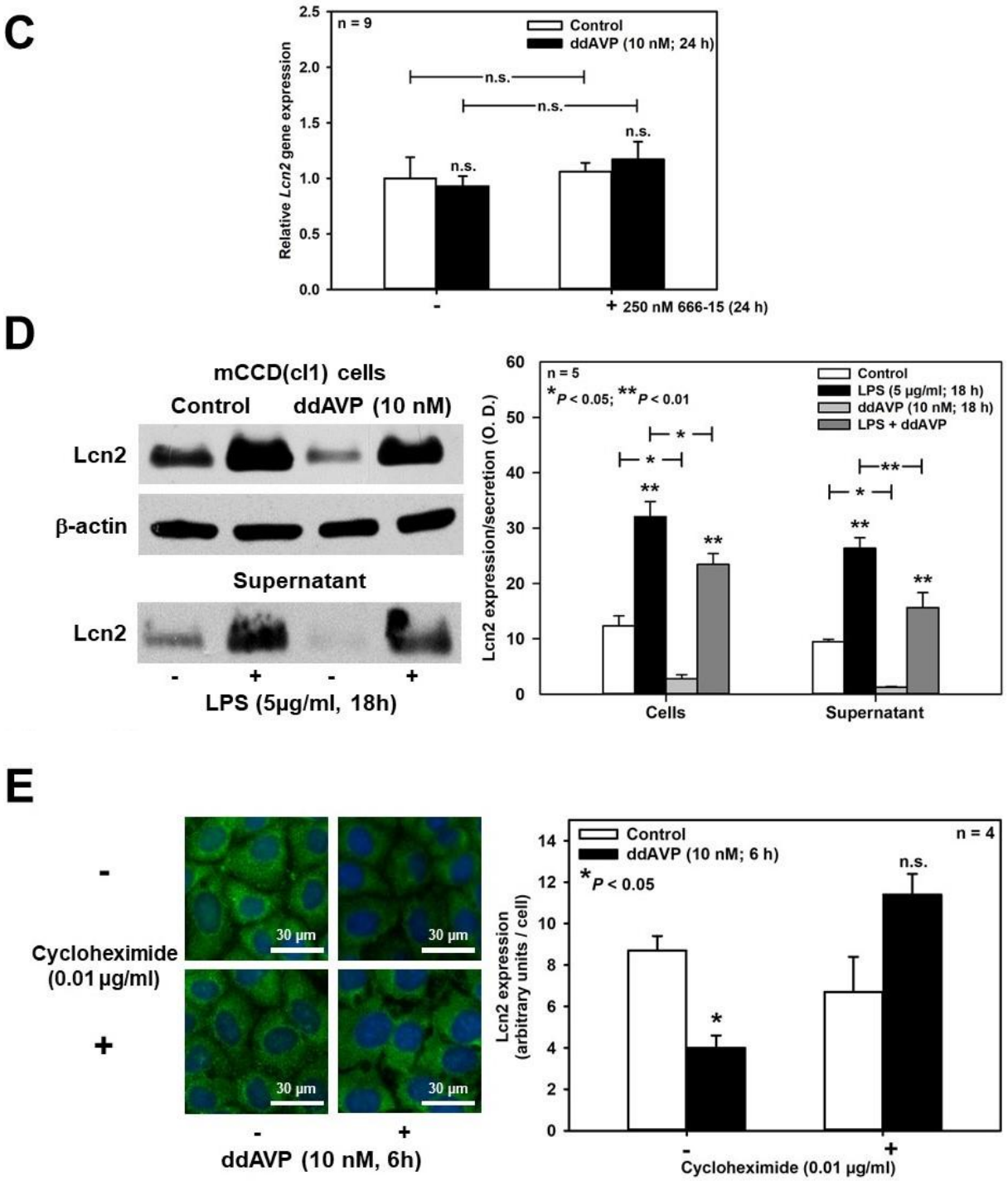

Figure 6. ddAVP decreases Lcn2 expression through a CREB-independent posttranslational mode of action in mCCD(cl.1) cells. (**A**, **B**) Expression levels of *Aqp2* (**A**) and *Lcn2* (**B**) mRNA by RT-PCR in mCCD(cl.1) cells treated with ddAVP ± LPS. Data are means ± SEM of 5-6 experiments. Statistical analysis compares expression levels of *Aqp2* or *Lcn2* in controls and ddAVP-treated cells ± LPS by one-way ANOVA. n.s. = not significant. (**C**) Expression levels of *Lcn2* mRNA by qPCR in mCCD(cl.1) cells treated with ddAVP ± 666-15. Data are means ± SEM of 9 experiments. Statistical analysis compares relative expression levels of *Lcn2* in controls and ddAVP-treated cells ± 666-15 by one-way ANOVA. n.s. = not significant. (**D**) Expression and secretion of Lcn2 in mCCD(cl.1) cells treated with LPS in the absence or presence of ddAVP. Media (supernatant) treated, as described in Figure 5E, were immunoblotted. Cellular Lcn2 protein expression was normalized to β-actin. Data are means ± SEM of 5 experiments. Statistical analysis compares expression levels of cellular and secreted Lcn2 in controls

and ddAVP-treated cells ± LPS by one-way ANOVA. **(E)** Expression of Lcn2 in mCCD(cl.1) cells treated with ddAVP for 6 h ± cycloheximide, a blocker of translational elongation, was detected by immunofluorescence microscopy of permeabilized cells. Hoechst 33342 counterstains nuclei. Statistical analysis shows means ± SEM of 4 experiments and comparison of the conditions ± ddAVP by unpaired *t*-test. n.s. = not significant.

Discussion

It is interesting to note that Slca22a17 regulation displays analogy to that of Aqp2 *in vivo* and in mpkCCDcl4 cells (reviewed in [3, 10]). AVP stimulation of PKA activity increases abundance of Aqp2by. PKA, in turn, activates AQP2 gene transcription in part via increased CREB binding to cis elements of the Aqp2 promoter. After longer periods of hypertonic challenge, Nfat5 also participates in increasing Aqp2 gene transcription. In contrast, bacterial infection has been shown to interfere with *Aqp2* mRNA and protein expression via activation of the inflammatory pathway involving NF-κB *in vivo* [38] and using LPS in cultured renal CCD mpkCCDcl4 [35]. Similarly, in mCCD(cl.1) cells, hyperosmolarity (Figure 1) and ddAVP (Figure 4A and 4B), respectively, increased Slc22a17 in a Nfat5- (Figures 3A and 3B) and CREB-dependent manner (Figures 4A and 4B), whereas LPS also reduced Slc22a17 expression (Figures 5A and 5B). The latter observation is similar to that of our previous study with mIMCD$_3$ cells where LPS reduced Slc22a17 expression as well [39], most likely via NF-κB activation [40].

In our previous study, mIMCD$_3$ cells activated Wnt/TCF1/β-catenin signaling with inhibitory phosphorylation of GSK-3β, which caused Slc22a17 upregulation, in response to hyperosmolarity [39]. *In silico* analysis [41, 42] indicated a putative TCF1 binding site 111 bases upstream of the *Slc22a17* gene, supporting the hypothesis that Slc22a17 is a downstream target of Wnt/β-catenin signaling. Is Wnt signaling linked to the central osmotic response pathway involving Nfat5? A study in HEK293 and mIMCD$_3$ cells indicated that inhibitory phosphorylation of GSK-3β contributes to high NaCl-induced activation of Nfat5 and suggested upstream regulation of Nfat5 by Wnt/GSK-3β signaling [43]. In support, a putative Nfat5 DNA consensus motif (osmotic response element (ORE) or tonicity-responsive enhancer (TonE)) [44] was identified in the human SLC22A17 promoter sequence ENSR00001455985/14:23820951-

23822367 ([828]AGGAAAATGCCA[839]), which is compatible with the data obtained in Figures 3A and 3B. It would be worthwhile to test this putative ORE in future experiments by site-directed mutagenesis of the sequence in a Slc22a17 luciferase-reporter gene assay. Moreover, a search of the Slc22a17 promoter sequence for CREB binding sites with the tools JASPAR and PROMO [41, 45] up to 2.7 kb upstream of the start codon yielded a putative binding site at position -736 (Ralf Zarbock and Frank Thévenod, *unpublished*), supporting the results obtained in Figure 4.

The human Lip2 gene (Ensembl ENSG00000148346; GenBank: X99133.1; 5869 bp) has 10 putative regulatory promoter sequences. Similarly, as described for Slc22a17, we have also identified a putative NFAT5 DNA binding sequence in a region of the human Lip2 gene ([841]TGGAAAAAGGCT[852]), which could explain Lip2 downregulation by hyperosmolarity in Figures 3C and 3D. In contrast, ddAVP did not influence Lcn2 gene expression (Figures 6B and 6C). Rather, ddAVP reduced Lcn2 protein expression by a posttranslational mechanism (Figures 6D and 6E).

It is interesting to note that Nfat5 regulates Lcn2 and its receptor Slc22a17 in an inverse manner, namely by causing upregulation of the receptor and downregulation of the ligand. In mIMCD$_3$ cells, hyperosmolarity induced an identical inverse regulation via Wnt/β-catenin signaling [39], possibly because Nfat5 is downstream of Wnt/GSK-3β signaling [43] (*see above*). In addition, the oncogene BCR-ABL activated the JAK/STAT pathway in murine myeloblast-like cells, which increased Lcn2, and repressed Lcn2-R expression in a Ras and Runx1-dependent manner [13, 46]. Hence, several signaling pathways exist to inversely control Lcn2 and its receptor, with different putative biological significance and outcomes (see below and [39] for a discussion).

Unexpectedly, the inverse regulation at the gene level did not extend to ddAVP-mediated CREB regulation. Whereas CREB activation increased Slc22a17, ddAVP

seemed to control Lcn2 via a posttranslational mechanism. For Aqp2, AVP not only regulates its expression at the gene level via CREB, but also PKA-dependent phosphorylation of the protein triggers its increased proteasomal and lysosomal degradation in a negative feed-back loop [47]. This is unlikely for Lcn2 because PKA does not phosphorylate the protein *in vitro* [48].

What could be the physiological significance of Slc22a17 upregulation in the context of hyperosmotic stress and AVP-mediated urinary concentration? Slc22a17 mediates receptor-mediated protein endocytosis in the distal nephron [14]. Endocytosed proteins are trafficked to lysosomes [14] where they are degraded. We speculate that Slc22a17 promotes osmotolerance by feeding cells with amino acids as precursors/osmolytes to maintain iso-osmolarity with the interstitium. However, this will require experimental proof. Downregulation of Lcn2 in the same context would also foster cellular protection during hyperosmotic stress. It has been proposed that Lcn2 upholds epithelial growth and proliferation (reviewed in [49]), which is associated with increased DNA replication and transcription. Osmotic stress induces DNA strand breaks, inhibits DNA repair and increases oxidative stress, which may all lead to increased mutation rates in dividing cells, unless proliferation is inhibited allowing for efficient repair.

Materials and Methods

Materials

Lipopolysaccharides (LPS) from Escherichia coli (cat. # L3129), [deamino-Cys1, D-Arg8]-vasopressin acetate salt hydrate (ddAVP, desmopressin) cat. # V1005) and protease inhibitor cocktail (cat. # P8340) were from Sigma-Aldrich. 3-(3-Aminopropoxy)-N-[2-[[3-[[(4-chloro-2-hydroxyphenyl) amino]carbonyl]-2-naphthalenyl] oxy] ethyl]-2-naphthalenecarboxamide hydrochloride (666-15) (cat. # 5661) was from Tocris Bioscience. Cycloheximide (cat. # ALX-380-269-G001) was from Enzo Life Sciences. All other reagents were of the highest purity grade possible. Materials were dissolved in water, ethanol, or dimethyl sulfoxide (DMSO). In control experiments, solvents were added to cells at concentrations not exceeding 0.2%. Antibodies are listed in Table 1.

Table 1. Primary antibodies.

Immunogen	Host species	Manufacturer	Catalog #	Application	Dilution
Rat Lcn2	goat	RD Biosystems	AF3508	IB	1:200-1:300
Mouse Lcn2	rabbit	Abcam	Ab63929	IF	1:250-1:1,000
Rat Slc22a17 (C-terminus)	rabbit	[14]	lg-1086	IB	1:100-1:2,000
Rat Slc22a17 (N-terminus)	rabbit	[14]	lg-1095	IF	1:100-1:1,000
Human β-actin	mouse	Sigma-Aldrich	A5316	IB	1:20,000
Human GAPDH (14C10)	mouse	Cell Signaling	2118	IB	1:20,000
Human Na^+,K^+-ATPase α1-subunit	rabbit	Cell Signaling	3010S	IB	1:250-1:500
Human Lamin A/C (4C11)	mouse	Cell Signaling	4777	IB	1:20,000
Human NFAT5	rabbit	[24]	N/A	IB	1:6,000

IB = immunoblotting; IF = immunofluorescence.

Methods

Culture of mCCD(cl.1) cells

The mouse (m)CCD(cl.1) cell line [50] was obtained from Dr. Edith Hummler (University of Lausanne, CH). Cells (passage 25-34) were cultured in Dulbecco's modified Eagle's medium (DMEM)/ nutrient mixture F-12 (1:1) (Gibco cat. # 31330) supplemented with 2.5 mM L-glutamine, 15 mM Hepes, 5% fetal bovine serum (FBS), 100 U/ml penicillin, and 100 µg/ml streptomycin, 0.9 µM insulin (Sigma-Aldrich; cat. # I1882), 5 µg/ml apo-transferrin (Sigma-Aldrich; cat. # T2252), 10 ng/ml EGF (Sigma-Aldrich; cat. # E9644), 1 nM T3 (Sigma-Aldrich; cat. # T6397), and 50 nM dexamethasone (Sigma-Aldrich; cat. # D4902) [51]. Cells were cultured in 25 cm^2 standard tissue culture flasks (Sarstedt) at 37°C in a humidified incubator with 5% CO_2, and passaging was performed twice a week upon reaching 90% confluency. Inhibitors (666-15, cycloheximide) were preincubated for 60 min.

Osmolarity/Tonicity experiments

Osmolarity is the measure of solute concentration per unit volume of solvent. Tonicity is the measure of the osmotic pressure gradient between two solutions across biological membranes. Unlike osmolarity, tonicity is only influenced by solutes that cannot cross this semipermeable membrane, because they create and influence the osmotic pressure gradient between the intracellular and extracellular compartments. Unless otherwise indicated in osmolarity/tonicity experiments, cell lines were cultured for 24 h in standard culture medium (= 300 mosmol/l) after seeding. Then medium was replaced with either normosmotic standard culture medium or hyperosmotic medium of 400 mosmol/l (by addition of 50 mmol/l NaCl from 3 M stock solutions), and cultured for up to 72 h. NaCl initially does not cross the cell membrane and therefore exerts an osmotic pressure gradient on the cells (hypertonicity). For simplification, the term "osmolarity" henceforth refers to osmolarity and tonicity.

Transient transfection

Cells were transiently transfected with *Nfat5* siRNA (sense primers for Stealth siRNA (Invitrogen, San Diego, CA) 5′-GGUGUUGCAGGUAUUUGUGGGCAAU-3′, 5′-GGAUUCUAUCAGGCCUGUAGAGUAA-3′, 5′-CCUAGUUCUCAAGAUCAGCAAGUAA-3′ [24]) or siRNA duplex negative control (Eurogentec cat. # SR-CL000-005). For lipid-based transfections, 1.0 x 10^5 mCCD(cl.1) cells were seeded in 6-well plates and transfected 24 h later at ~40% confluence with 5 nM siRNA using Lipofectamine RNAiMAX (Thermo Fisher Scientific) according to manufacturer's instructions. After 24 h, the medium was exchanged to 300 or 400 mosmol/l media.

Transfection by electroporation was performed as described previously [52], with slight modifications. Briefly, 2.0 x 10^6 mCCD(cl.1) cells were electroporated at 300 mV and 960 µF using a Bio-Rad Gene Pulser and transfected with 100-250 nM siRNA. For osmolarity experiments, 1 x 10^6 electroporated cells were seeded in 25 cm^2 flasks or 2 x 10^4 cells seeded on glass cover slips.

RNA extraction, cDNA synthesis and reverse transcription PCR (RT-PCR)

Isolation of total RNA, synthesis of cDNA and PCR reactions were performed as previously described [39, 53]. PCR reactions were performed using specific primers and cycling protocols (Table 2). Gel documentation and densitometry analysis were performed using Image Lab Software version 5.2 (Bio-Rad Laboratories) with correction for loading with the housekeeping gene glyceraldehyde-3-phosphate dehydrogenase (*Gapdh)*.

Preprints (www.preprints.org) | NOT PEER-REVIEWED | Posted: 4 September 2019 doi:10.20944/preprints201909.0047.v1

Peer-reviewed version available at Int. J. Mol. Sci. 2019, 20, 5398; doi:10.3390/ijms20215398

Table 2. Protocols for reverse transcription-PCR.

	Gapdh	*Aqp2*	*Lcn2*	*Slc22a17*
Accession number	NM_001289726.1	NM_009699.3	NM_008491.1	NM_021551.4
Forward primer (5' - 3')	AGGGCTCATGACCACAGT	TGGCTGTCAATGCTCTCCAC	CCACCACGGACTACAACCAG	CAGCCACCTCCTAACCGCTGTG
Reverse primer (5' - 3')	TGCAGGGATGATGTTCTG	GGAGCAGCCGGTGAAATAGA	AGCTCCTTGGTTCTTCCATACA	CTCCCACTAGGCTCAAAGGCTGCT
Reference	NCBI Primer-BLAST	[53]	[39]	[39]
Activation	5 min 95°C	5 min 95°C	5 min 95°C	5 min 95°C
Cycle number	18-22	31-33	20-25	27-29
Denaturation	30 sec 94°C	30 sec 94°C	30 sec 94°C	30 sec 94°C
Annealing	30 sec 60°C	30 sec 62°C	30 sec 60°C	30 sec 60°C
Extension	30 sec 72°C	30 sec 72°C	30 sec 72°C	30 sec 72°C
Final Extension	7 min 72°C	7 min 72°C	7 min 72°C	7 min 72°C
PCR product (bp)	112	200	100	86

Quantitative PCR (qPCR)

RNA extraction and cDNA synthesis were performed as described for the RT-PCR protocol. Primers were designed using PrimerBLAST software (NCBI) and/or taken from the literature. The primers were obtained from Eurofins Genomics (Table 3) and tested for primer efficiency using serially diluted cDNA (see Table3). Quantitative PCR (qPCR) was performed essentially as described [39, 54] in a StepOnePlus Real-Time PCR System (Applied Biosystems) using KAPA SYBR FAST qPCR Master Mix Universal and High ROX Reference Dye (Roche). The cycling conditions were activation at 95 °C for 5 min, 40 cycles (42 cycles for *Aqp2*) of 95 °C for 3 s and 60 °C (62 °C for *Aqp2*) for 30 s with melt curve analysis to check amplification specificity. Gene expression levels were calculated according to the $2^{-\Delta Cq}$ method relative to the sample with the highest expression (minimum *Cq*) [55]. The data obtained were normalized to the expression of two stable reference genes: *Gapdh* and β-actin (*Actb*).

Table 3. qPCR primers.

Gene-name (Accession number)	Forward (5' - 3')	Reverse (5' - 3')	Reference	Amplicon size (bp)	Efficiency (%)
Actb (NM_007393.5)	CGTGCGTGACATCAAAGAGAA	GGCCATCTC CTGCTCGAA	[39]	61	102
Gapdh (NM_001289726.1)	CGGCCGCATCTTCTTGTG	CCGACCTTCACCATTTTGTCTAC	[39]	59	100
Lcn2 (NM_008491.1)	CCACCACGGACTACAACCAG	AGCTCCTTGGTTCTTCCATACA	[39]	100	98
Slc22a17 (NM_021551.4)	CAGCCACCTCCTAACCGCTGTG	CTCCCACTAGGCTCAAAGGCTGCT	[39]	86	110
Aqp2 (NM_009699.3)	TGGCTGTCAATGCTCTCCAC	GGAGCAGCCGGTGAAATAGA	[53]	200	92

Measurements of transepithelial electrical resistance (TEER) of cell monolayers

Cells (2 x 10^4) were plated in transwell filters for 24-well plates with 0.4-µm pore size and 0.33-cm^2 surface area (cat. # 3470, Costar Transwell-Clear, Corning). After two days, transepithelial electrical resistance (TEER) was measured daily using an epithelial volt-ohm meter EVOM with an STX2 electrode (World Precision Instruments) at room temperature. Reported resistance readings were corrected for background by subtracting the resistance of empty cell-free inserts in culture medium of 140.3 ± 4.0 Ω (means ± SEM; n = 17). Treatments were started 14-15 days after seeding, when TEER reached a stable value of 284.3 ± 15.9 Ω x cm^2 (means ± SEM; n = 17). LPS and/or ddAVP were then added to both the apical (upper chamber, 300 µl medium) and basolateral (lower chamber, 1000 µl medium) compartments and incubated for 18 h at 37°C, prior to measurements of Lcn2 expression and secretion.

Determination of Lcn2 expression and secretion

Lcn2 secretion by mCCD(cl.1) cells was detected by immunoblotting. Media from the apical and basolateral compartments of transwell filters were concentrated at room temperature to a final volume of 100-150 µl using Vivaspin 500 centrifugal concentrators (10 kDa molecular weight cut-off; cat. # VS0102, Sartorius), corrected for volume differences and used for immunoblotting. To determine cellular Lcn2

expression, cells grown on filters were lysed in 30 µl/well of lysis buffer (25 mM Tris pH 7.4, 2 mM Na_3VO_4, 10 mM NaF, 10 mM $Na_4P_2O_7$, 1 mM ethylenediaminetetraacetic acid (EDTA), 1 mM ethylene glycol-bis(β-aminoethyl ether)-N,N,N',N'-tetraacetic acid (EGTA), 1% Nonidet P-40) containing protease inhibitors. For Lcn2 expression by RT-PCR, cells grown on transwell filters were washed once with phosphate buffered saline (PBS), and collected by scraping in 100 µl PBS using a rubber policeman.

Isolation of plasma membrane enriched microsomes

2 x 10^6 mCCD(cl.1) cells were seeded into 175 cm^2 culture flasks and grown for 24 h in standard culture medium before osmotic challenge for 72 h. Plasma membranes were obtained by differential ultracentrifugation at 4 °C. Cells were homogenized by nitrogen pressure cavitation in a Parr Instruments 45-ml cell disruption vessel (Moline, IL) for 2 min at 1000 p.s.i. To remove unbroken cells, nuclei, large debris and mitochondria, homogenate was centrifuged at 8000 x *g* for 20 min, and the resulting supernatant was centrifuged for 45 min at 35,000 x *g* to yield a microsomal fraction in the pellet, resuspended and supplemented with protease inhibitors. Plasma membrane purity was verified by immunoblotting and showed about 10-fold enrichment of Na^+,K^+-ATPase (Figure 1C).

Isolation of nuclei

4 x 10^5 cells were plated into 75 cm^2 culture flasks and grown for 48 h to reach a confluency of ~80% before medium was replaced by 300-500 mosmol/l media and incubation for additional 24 h. Nuclei and post-nuclear supernatant were separated as reported elsewhere [56]. All steps were performed at 4°C. Cells were swelled in hypotonic buffer A (10 mM HEPES-KOH, pH 7.9, 1.5 mM $MgCl_2$, 10 mM KCl, 0.5 mM dithiothreitol (DTT), 0.05% Nonidet P-40) containing protease inhibitors, Tenbroeck homogenized, and nuclei were pelleted (220 x *g*, 5 min). Nuclei were washed with

buffer A + 0.3% Nonidet P-40 to remove cytoplasmic contaminants and pelleted (600 x *g*, 5 min). Nuclei were resuspended in 0.25 M sucrose/10 mM $MgCl_2$, layered over 0.35 M sucrose/0.5 mM $MgCl_2$ and centrifuged at 1,430 x *g* for 5 min. Purified nuclei were stored in buffer B (20 mM HEPES-KOH, pH 7.9, 25% glycerol, 420 mM NaCl, 1.5 mM $MgCl_2$, 0.2 mM EDTA, 0.5 mM DTT, 0.05% Nonidet P-40) containing protease inhibitors. Samples were sonicated using a Branson Digital Sonifier (3 x 5s at 20% output) prior to protein determination by the Bradford method [57], using bovine serum albumin (BSA) as a standard.

Immunoblotting

Sodium dodecyl sulfate polyacrylamide gel electrophoresis (SDS-PAGE) and immunoblotting were essentially performed according to standard procedures by wet transfer, as described earlier [14], with the exception of Lcn2 immunoblots that were electroblotted by rapid semi-dry transfer (Bio-Rad Laboratories Trans-Blot Turbo). Cells were washed in PBS, scraped and homogenized by sonication in isosmotic sucrose buffer. Protein concentration was determined by the Bradford method [57]. Equal amounts of protein (5-30 µg) were subjected to SDS-PAGE and immunoblotted. Primary antibodies and their dilutions are listed in Table 1. Horseradish peroxidase-conjugated secondary antibodies were purchased from Santa Cruz Biotechnology, Inc. or GE Healthcare and used at 1:2500 – 1:30,000 dilutions. Densitometry analysis was performed using ImageJ software [58].

Immunofluorescence staining and microscopy

mCCD(cl.1) cells (0.5-2.0 x 10^4 cells / well) were plated on glass coverslips and cultured for 24-72 h to reach a confluence of 40-50% prior to treatments.

For surface staining (at 4°C), cells were blocked with 1% BSA-PBS for 1 h followed by incubation with rabbit polyclonal antibody against N-terminal rodent anti-

Lcn2-R polyclonal rabbit IgG (1:100 dilution in 1% BSA-PBS ≡ 10 µg/ml) for 2 h. Cells were then incubated with secondary Alexa Fluor 488-conjugated goat anti-rabbit IgG (1:600; cat. # A-11008, Thermo Fisher) for 1 h and fixed with 4% paraformaldehyde (PFA) in PBS for 30 min at room temperature. Nuclei were counterstained with 0.8 µg/ml Hoechst 33342 for 5 min. Coverslips were embedded with DAKO fluorescent mounting medium, and images were acquired as described elsewhere [59].

For total cellular Lcn2-R staining at room temperature (LPS experiments), cells were fixed with 4% PFA in PBS for 30 min, permeabilized with 1% SDS in PBS for 15 min, and blocked with 1% BSA-PBS for 40 min. N-terminal rodent anti-Lcn2-R polyclonal rabbit IgG (1:100-1,000 dilution in 1% BSA-PBS) was incubated for 2 h. Subsequent steps were identical to surface staining procedures.

Statistics

Unless otherwise indicated, the experiments were always repeated at least three times with independent cultures. Means ± SEM are shown. Statistical analysis using unpaired Student's *t*-test was carried out with GraphPad Prism v. 5.01 (GraphPad Software Inc., San Diego California USA). For more than two groups, one-way ANOVA with Tukey or Dunnett's post hoc test assuming equality of variance was applied. Results with $P < 0.05$ were considered to be statistically significant.

Conclusions

In summary, the present study unveils a signaling mechanism involved in the regulation of the expression of the Lcn2 receptor Slc22a17 by hyperosmolarity in the cultured CCD cell line mCCD(cl.1) via Nfat5 and by AVP via CREB, which parallels Aqp2 regulation, suggesting a role of Slc22a17 in adaptation to osmotic stress. In contrast, the ligand of Slc22a17, Lcn2 is downregulated by hyperosmolarity and AVP in a Nfat5-dependent, CREB-independent manner. Rather, PKA-dependent posttranslational control of Lcn2 occurs via ill-defined mechanisms. We speculate that Lcn2 downregulation may prevent increased proliferation and permanent damage of osmotically stressed cells.

Acknowledgments

This work was supported by the Deutsche Forschungsgemeinschaft (DFG TH345/11-1), a BMBF grant between Germany and Mexico (BMBF 01DN16039), and the Centre for Biomedical Training and Research (ZBAF) of the University of Witten/Herdecke. The authors are grateful to Drs. Hyug Moo Kwon (Ulsan National Institute of Science and Technology, School of Nano-Bioscience and Chemical Engineering; Ulsan, South Korea) and Eric Feraille (University of Geneva, Department of Cellular Physiology and Metabolism, Geneva, Switzerland) for permission to use their Nfat5 plasmids, antibodies and siRNAs. The authors thank Dr. Johannes Fels (Physiology, Witten/Herdecke University) for valuable discussions.

Conflict of Interests

The authors declare that they have no conflict of interests.

Data availability statement

The data sets used and/or analyzed during the current study are available from the corresponding author on reasonable request.

Author Contributions

Conceptualization, Frank Thévenod; Formal analysis, Stephanie Probst, Bettina Scharner and Frank Thévenod; Funding acquisition, Frank Thévenod; Investigation, Wing-Kee Lee and Frank Thévenod; Methodology, Stephanie Probst and Bettina Scharner; Project administration, Bettina Scharner and Frank Thévenod; Supervision, Wing-Kee Lee and Frank Thévenod; Validation, Wing-Kee Lee and Frank Thévenod; Visualization, Stephanie Probst and Frank Thévenod; Writing – original draft, Frank Thévenod; Writing – review & editing, Stephanie Probst, Bettina Scharner, Wing-Kee Lee and Frank Thévenod.

References

1. Knepper, M. A.; Hoffert, J. D.; Packer, R. K.; Fenton, R. A., Urine Concentration and Dilution. In *Brenner & Rector's The Kidney*, 8 ed.; Brenner, B. M., Ed. Saunders: Philadelphia, 2008; Vol. 1, pp 308-329.
2. Brown, D.; Nielsen, S., Cell Biology of Vasopressin Action. In *Brenner & Rector's The Kidney*, 8 ed.; Brenner, B. M., Ed. Saunders: Philadelphia, 2008; Vol. 1.
3. Hasler, U.; Leroy, V.; Martin, P. Y.; Feraille, E., Aquaporin-2 abundance in the renal collecting duct: new insights from cultured cell models. *Am J Physiol Renal Physiol* **2009,** 297, F10-8.
4. Hozawa, S.; Holtzman, E. J.; Ausiello, D. A., cAMP motifs regulating transcription in the aquaporin 2 gene. *Am J Physiol* **1996,** 270, C1695-702.
5. Matsumura, Y.; Uchida, S.; Rai, T.; Sasaki, S.; Marumo, F., Transcriptional regulation of aquaporin-2 water channel gene by cAMP. *J Am Soc Nephrol* **1997,** 8, 861-7.
6. Yasui, M.; Zelenin, S. M.; Celsi, G.; Aperia, A., Adenylate cyclase-coupled vasopressin receptor activates AQP2 promoter via a dual effect on CRE and AP1 elements. *Am J Physiol* **1997,** 272, F443-50.
7. Ullrich, K. J.; Drenckhahn, F. O.; Jarausch, K. H., [Studies on the problem of urine concentration and dilution; osmotic behavior of renal cells and accompanying electrolyte accumulation in renal tissue in various diuretic conditions]. *Pflugers Archiv fur die gesamte Physiologie des Menschen und der Tiere* **1955,** 261, 62-77.
8. Jarausch, K. H.; Ullrich, K. J., [Studies on the problem of urine concentration and dilution; distribution of electrolytes (sodium, potassium, calcium, magnesium, anorganic phosphate), urea amino acids and exogenous creatinine

in the cortex and medulla of dog kidney in various diuretic conditions]. *Pflugers Archiv fur die gesamte Physiologie des Menschen und der Tiere* **1956,** 262, 537-50.

9. Burg, M. B.; Ferraris, J. D.; Dmitrieva, N. I., Cellular response to hyperosmotic stresses. *Physiol Rev* **2007,** 87, 1441-74.
10. Hasler, U., Controlled aquaporin-2 expression in the hypertonic environment. *Am J Physiol Cell Physiol* **2009,** 296, C641-53.
11. Abergel, R. J.; Clifton, M. C.; Pizarro, J. C.; Warner, J. A.; Shuh, D. K.; Strong, R. K.; Raymond, K. N., The siderocalin/enterobactin interaction: a link between mammalian immunity and bacterial iron transport. *Journal of the American Chemical Society* **2008,** 130, 11524-34.
12. Paragas, N.; Kulkarni, R.; Werth, M.; Schmidt-Ott, K. M.; Forster, C.; Deng, R.; Zhang, Q.; Singer, E.; Klose, A. D.; Shen, T. H.; Francis, K. P.; Ray, S.; Vijayakumar, S.; Seward, S.; Bovino, M. E.; Xu, K.; Takabe, Y.; Amaral, F. E.; Mohan, S.; Wax, R.; Corbin, K.; Sanna-Cherchi, S.; Mori, K.; Johnson, L.; Nickolas, T.; D'Agati, V.; Lin, C. S.; Qiu, A.; Al-Awqati, Q.; Ratner, A. J.; Barasch, J., alpha-Intercalated cells defend the urinary system from bacterial infection. *J Clin Invest* **2014,** 124, 2963-76.
13. Devireddy, L. R.; Gazin, C.; Zhu, X.; Green, M. R., A cell-surface receptor for lipocalin 24p3 selectively mediates apoptosis and iron uptake. *Cell* **2005,** 123, 1293-1305.
14. Langelueddecke, C.; Roussa, E.; Fenton, R. A.; Wolff, N. A.; Lee, W. K.; Thévenod, F., Lipocalin-2 (24p3/neutrophil gelatinase-associated lipocalin (NGAL)) receptor is expressed in distal nephron and mediates protein endocytosis. *J Biol Chem* **2012,** 287, 159-169.

15. Dizin, E.; Hasler, U.; Nlandu-Khodo, S.; Fila, M.; Roth, I.; Ernandez, T.; Doucet, A.; Martin, P. Y.; Feraille, E.; de Seigneux, S., Albuminuria induces a proinflammatory and profibrotic response in cortical collecting ducts via the 24p3 receptor. *Am J Physiol Renal Physiol* **2013,** 305, F1053-F1063.

16. Thévenod, F.; Wolff, N. A., Iron transport in the kidney: implications for physiology and cadmium nephrotoxicity. *Metallomics : integrated biometal science* **2016,** 8, 17-42.

17. Thévenod, F.; Fels, J.; Lee, W. K.; Zarbock, R., Channels, transporters and receptors for cadmium and cadmium complexes in eukaryotic cells: myths and facts. *Biometals* **2019,** 32, 469-489.

18. Christensen, E. I.; Birn, H., Megalin and cubilin: multifunctional endocytic receptors. *Nat Rev Mol Cell Biol* **2002,** 3, 256-266.

19. Lee, J. W.; Chou, C. L.; Knepper, M. A., Deep Sequencing in Microdissected Renal Tubules Identifies Nephron Segment-Specific Transcriptomes. *J Am Soc Nephrol* **2015,** 26, 2669-77.

20. Betten, R.; Langelueddecke, C.; Edemir, B.; Thévenod, F., Regulation of 24p3 and 24p3 receptor expression by tonicity in rodent renal inner medullary collecting duct cells: Possible involvement of Wnt/beta-catenin signaling. *Acta Physiol Scand* **2013,** 207, (S694), 180 (S694; abstract)

21. Cabedo Martinez, A. I.; Weinhaupl, K.; Lee, W. K.; Wolff, N. A.; Storch, B.; Zerko, S.; Konrat, R.; Kozminski, W.; Breuker, K.; Thévenod, F.; Coudevylle, N., Biochemical and Structural Characterization of the Interaction between the Siderocalin NGAL/LCN2 (Neutrophil Gelatinase-associated Lipocalin/Lipocalin 2) and the N-terminal Domain of Its Endocytic Receptor SLC22A17. *J Biol Chem* **2016,** 291, 2917-30.

22. Marples, D.; Christensen, B. M.; Frokiaer, J.; Knepper, M. A.; Nielsen, S., Dehydration reverses vasopressin antagonist-induced diuresis and aquaporin-2 downregulation in rats. *Am J Physiol* **1998,** 275, F400-9.

23. Preisser, L.; Teillet, L.; Aliotti, S.; Gobin, R.; Berthonaud, V.; Chevalier, J.; Corman, B.; Verbavatz, J. M., Downregulation of aquaporin-2 and -3 in aging kidney is independent of V(2) vasopressin receptor. *Am J Physiol Renal Physiol* **2000,** 279, F144-52.

24. Hasler, U.; Jeon, U. S.; Kim, J. A.; Mordasini, D.; Kwon, H. M.; Feraille, E.; Martin, P. Y., Tonicity-responsive enhancer binding protein is an essential regulator of aquaporin-2 expression in renal collecting duct principal cells. *J Am Soc Nephrol* **2006,** 17, 1521-31.

25. Sheen, M. R.; Kim, J. A.; Lim, S. W.; Jung, J. Y.; Han, K. H.; Jeon, U. S.; Park, S. H.; Kim, J.; Kwon, H. M., Interstitial tonicity controls TonEBP expression in the renal medulla. *Kidney Int* **2009,** 75, 518-25.

26. Ko, B. C.; Turck, C. W.; Lee, K. W.; Yang, Y.; Chung, S. S., Purification, identification, and characterization of an osmotic response element binding protein. *Biochem Biophys Res Commun* **2000,** 270, 52-61.

27. Miyakawa, H.; Woo, S. K.; Dahl, S. C.; Handler, J. S.; Kwon, H. M., Tonicity-responsive enhancer binding protein, a rel-like protein that stimulates transcription in response to hypertonicity. *Proc Natl Acad Sci U S A* **1999,** 96, 2538-42.

28. DiGiovanni, S. R.; Nielsen, S.; Christensen, E. I.; Knepper, M. A., Regulation of collecting duct water channel expression by vasopressin in Brattleboro rat. *Proc Natl Acad Sci U S A* **1994,** 91, 8984-8.

29. Hayashi, M.; Sasaki, S.; Tsuganezawa, H.; Monkawa, T.; Kitajima, W.; Konishi, K.; Fushimi, K.; Marumo, F.; Saruta, T., Expression and distribution of aquaporin

of collecting duct are regulated by vasopressin V2 receptor in rat kidney. *J Clin Invest* **1994,** 94, 1778-83.

30. Hasler, U.; Mordasini, D.; Bens, M.; Bianchi, M.; Cluzeaud, F.; Rousselot, M.; Vandewalle, A.; Feraille, E.; Martin, P. Y., Long term regulation of aquaporin-2 expression in vasopressin-responsive renal collecting duct principal cells. *J Biol Chem* **2002,** 277, 10379-86.
31. Schenk, L. K.; Bolger, S. J.; Luginbuhl, K.; Gonzales, P. A.; Rinschen, M. M.; Yu, M. J.; Hoffert, J. D.; Pisitkun, T.; Knepper, M. A., Quantitative proteomics identifies vasopressin-responsive nuclear proteins in collecting duct cells. *J Am Soc Nephrol* **2012,** 23, 1008-18.
32. Xie, F.; Li, B. X.; Kassenbrock, A.; Xue, C.; Wang, X.; Qian, D. Z.; Sears, R. C.; Xiao, X., Identification of a Potent Inhibitor of CREB-Mediated Gene Transcription with Efficacious in Vivo Anticancer Activity. *J Med Chem* **2015,** 58, 5075-87.
33. Takeuchi, O.; Hoshino, K.; Kawai, T.; Sanjo, H.; Takada, H.; Ogawa, T.; Takeda, K.; Akira, S., Differential roles of TLR2 and TLR4 in recognition of gram-negative and gram-positive bacterial cell wall components. *Immunity* **1999,** 11, 443-51.
34. Wolfs, T. G.; Buurman, W. A.; van Schadewijk, A.; de Vries, B.; Daemen, M. A.; Hiemstra, P. S.; van 't Veer, C., In vivo expression of Toll-like receptor 2 and 4 by renal epithelial cells: IFN-gamma and TNF-alpha mediated up-regulation during inflammation. *J Immunol* **2002,** 168, 1286-93.
35. Hasler, U.; Leroy, V.; Jeon, U. S.; Bouley, R.; Dimitrov, M.; Kim, J. A.; Brown, D.; Kwon, H. M.; Martin, P. Y.; Feraille, E., NF-kappaB modulates aquaporin-2 transcription in renal collecting duct principal cells. *J Biol Chem* **2008,** 283, 28095-105.

36. Cowland, J. B.; Borregaard, N., Molecular characterization and pattern of tissue expression of the gene for neutrophil gelatinase-associated lipocalin from humans. *Genomics* **1997,** 45, 17-23.

37. Schneider-Poetsch, T.; Ju, J.; Eyler, D. E.; Dang, Y.; Bhat, S.; Merrick, W. C.; Green, R.; Shen, B.; Liu, J. O., Inhibition of eukaryotic translation elongation by cycloheximide and lactimidomycin. *Nat Chem Biol* **2010,** 6, 209-217.

38. Hocherl, K.; Schmidt, C.; Kurt, B.; Bucher, M., Inhibition of NF-kappaB ameliorates sepsis-induced downregulation of aquaporin-2/V2 receptor expression and acute renal failure in vivo. *Am J Physiol Renal Physiol* **2010,** 298, F196-204.

39. Betten, R.; Scharner, B.; Probst, S.; Edemir, B.; Wolff, N. A.; Langelueddecke, C.; Lee, W. K.; Thévenod, F., Tonicity inversely modulates lipocalin-2 (Lcn2/24p3/NGAL) receptor (SLC22A17) and Lcn2 expression via Wnt/beta-catenin signaling in renal inner medullary collecting duct cells: implications for cell fate and bacterial infection. *Cell Commun Signal* **2018,** 16, 74.

40. Kuper, C.; Beck, F. X.; Neuhofer, W., Toll-like receptor 4 activates NF-kappaB and MAP kinase pathways to regulate expression of proinflammatory COX-2 in renal medullary collecting duct cells. *Am J Physiol Renal Physiol* **2012,** 302, F38-46.

41. Messeguer, X.; Escudero, R.; Farre, D.; Nunez, O.; Martinez, J.; Alba, M. M., PROMO: detection of known transcription regulatory elements using species-tailored searches. *Bioinformatics* **2002,** 18, 333-4.

42. Farre, D.; Roset, R.; Huerta, M.; Adsuara, J. E.; Rosello, L.; Alba, M. M.; Messeguer, X., Identification of patterns in biological sequences at the ALGGEN server: PROMO and MALGEN. *Nucleic Acids Res* **2003,** 31, 3651-3.

43. Zhou, X.; Wang, H.; Burg, M. B.; Ferraris, J. D., Inhibitory phosphorylation of GSK-3beta by AKT, PKA, and PI3K contributes to high NaCl-induced activation of the transcription factor NFAT5 (TonEBP/OREBP). *Am J Physiol Renal Physiol* **2013,** 304, F908-17.

44. Ferraris, J. D.; Williams, C. K.; Ohtaka, A.; Garcia-Perez, A., Functional consensus for mammalian osmotic response elements. *Am J Physiol* **1999,** 276, C667-73.

45. Khan, A.; Fornes, O.; Stigliani, A.; Gheorghe, M.; Castro-Mondragon, J. A.; van der Lee, R.; Bessy, A.; Cheneby, J.; Kulkarni, S. R.; Tan, G.; Baranasic, D.; Arenillas, D. J.; Sandelin, A.; Vandepoele, K.; Lenhard, B.; Ballester, B.; Wasserman, W. W.; Parcy, F.; Mathelier, A., JASPAR 2018: update of the open-access database of transcription factor binding profiles and its web framework. *Nucleic Acids Res* **2018,** 46, D260-D266.

46. Sheng, Z.; Wang, S. Z.; Green, M. R., Transcription and signalling pathways involved in BCR-ABL-mediated misregulation of 24p3 and 24p3R. *EMBO J* **2009,** 28, 866-76.

47. Hasler, U.; Nielsen, S.; Feraille, E.; Martin, P. Y., Posttranscriptional control of aquaporin-2 abundance by vasopressin in renal collecting duct principal cells. *Am J Physiol Renal Physiol* **2006,** 290, F177-87.

48. Lee, Y. C.; Lin, S. D.; Yu, H. M.; Chen, S. T.; Chu, S. T., Phosphorylation of the 24p3 protein secreted from mouse uterus in vitro and in vivo. *J Protein Chem* **2001,** 20, (7), 563-9.

49. Correnti, C.; Strong, R. K., Mammalian siderophores, siderophore-binding lipocalins, and the labile iron pool. *J Biol Chem* **2012,** 287, 13524-31.

50. Gaeggeler, H. P.; Gonzalez-Rodriguez, E.; Jaeger, N. F.; Loffing-Cueni, D.; Norregaard, R.; Loffing, J.; Horisberger, J. D.; Rossier, B. C., Mineralocorticoid

versus glucocorticoid receptor occupancy mediating aldosterone-stimulated sodium transport in a novel renal cell line. *J Am Soc Nephrol* **2005,** 16, 878-91.

51. Fila, M.; Brideau, G.; Morla, L.; Cheval, L.; Deschenes, G.; Doucet, A., Inhibition of K+ secretion in the distal nephron in nephrotic syndrome: possible role of albuminuria. *J Physiol* **2011,** 589, 3611-21.

52. Mordasini, D.; Bustamante, M.; Rousselot, M.; Martin, P. Y.; Hasler, U.; Feraille, E., Stimulation of Na+ transport by AVP is independent of PKA phosphorylation of the Na-K-ATPase in collecting duct principal cells. *Am J Physiol Renal Physiol* **2005,** 289, F1031-9.

53. Moeller, H. B.; Slengerik-Hansen, J.; Aroankins, T.; Assentoft, M.; MacAulay, N.; Moestrup, S. K.; Bhalla, V.; Fenton, R. A., Regulation of the Water Channel Aquaporin-2 via 14-3-3theta and -zeta. *J Biol Chem* **2016,** 291, 2469-84.

54. Nair, A. R.; Lee, W. K.; Smeets, K.; Swennen, Q.; Sanchez, A.; Thévenod, F.; Cuypers, A., Glutathione and mitochondria determine acute defense responses and adaptive processes in cadmium-induced oxidative stress and toxicity of the kidney. *Arch Toxicol* **2015,** 89, 2273-89.

55. Bustin, S. A.; Benes, V.; Garson, J. A.; Hellemans, J.; Huggett, J.; Kubista, M.; Mueller, R.; Nolan, T.; Pfaffl, M. W.; Shipley, G. L.; Vandesompele, J.; Wittwer, C. T., The MIQE guidelines: minimum information for publication of quantitative real-time PCR experiments. *Clin Chem* **2009,** 55, 611-22.

56. Lam, Y. W.; Lamond, A. I., Isolation of nucleoli. In *Cell Biology: A Laboratory Handbook; Third Edition*, 3 ed.; Celis, J. E., Ed. Elsevier Academic Press: Burlington, MA, 2006; Vol. 2, pp 103–108.

57. Bradford, M. M., A rapid and sensitive method for the quantitation of microgram quantities of protein utilizing the principle of protein-dye binding. *Anal Biochem* **1976,** 72, 248-254.

58. Schneider, C. A.; Rasband, W. S.; Eliceiri, K. W., NIH Image to ImageJ: 25 years of image analysis. *Nat Methods* **2012,** 9, 671-5.

59. Wolff, N. A.; Abouhamed, M.; Verroust, P. J.; Thévenod, F., Megalin-dependent internalization of cadmium-metallothionein and cytotoxicity in cultured renal proximal tubule cells. *J Pharmacol Exp Ther* **2006,** 318, 782-791.